

**DOT/FAA/TC-20/35**

Federal Aviation Administration  
William J. Hughes Technical Center  
Aviation Research Division  
Atlantic City International Airport  
New Jersey 08405

# **A Physical Basis for Comparing Flammability of Aircraft Cabin Materials Using a Microscale Combustion Calorimeter**

August, 2020

Final report



U.S. Department of Transportation  
**Federal Aviation Administration**

## NOTICE

This document is disseminated under the sponsorship of the U.S. Department of Transportation in the interest of information exchange. The U.S. Government assumes no liability for the contents or use thereof. The U.S. Government does not endorse products or manufacturers. Trade or manufacturers' names appear herein solely because they are considered essential to the objective of this report. The findings and conclusions in this report are those of the author(s) and do not necessarily represent the views of the funding agency. This document does not constitute FAA policy. Consult the FAA sponsoring organization listed on the Technical Documentation page as to its use.

This report is available at the Federal Aviation Administration William J. Hughes Technical Center's Full-Text Technical Reports page: [actlibrary.tc.faa.gov](http://actlibrary.tc.faa.gov) in Adobe Acrobat portable document format (PDF).

Form DOT F 1700.7 (8-72)

Reproduction of completed page authorized

1. Report No. DOT/FAA/TC-20/35		2. Government Accession No.		3. Recipient's Catalog No.	
4. Title and Subtitle A Physical Basis for Comparing Flammability of Aircraft Cabin Materials Using a Microscale Combustion Calorimeter				5. Report Date August 2020	
				6. Performing Organization Code	
7. Author(s) Richard E. Lyon, Natallia Safronava, Sean Crowley, and Richard N. Walters				8. Performing Organization Report No.	
9. Performing Organization Name and Address Federal Aviation Administration Fire Safety Branch, Aviation Research Division William J. Hughes Technical Center, Atlantic City Airport, NJ 08405				10. Work Unit No. (TRAIS)	
				11. Contract or Grant No.	
12. Sponsoring Agency Name and Address U.S. Department of Transportation FAA Northwest Mountain Regional Office 1601 Lind Avenue SW Renton, WA 98057				13. Type of Report and Period Covered Technical Report	
				14. Sponsoring Agency Code AIR-600	
15. Supplementary Notes					
16. Abstract  In this study, a burning model is used to link the molecular-level processes of flaming combustion measured in thermal analysis to the fire response of a polymer at the continuum level. A flammability parameter that includes ignitability and burning rate, driven by heat release, emerging from this analysis is called the Fire Growth Capacity ( <i>FGC</i> ). The <i>FGC</i> was measured in a micro ( $10^{-6}$ kg) scale combustion calorimeter for 30 polymers, and successfully ranked the expected fire performance of these polymers in bench (kg) scale flame and fire tests.					
17. Key Words Fire response, burning model, isokinetic temperature, ignition temperature, burning temperature, fire growth capacity, microscale combustion calorimeter, fire tests			18. Distribution Statement This document is available to the U.S. public through the National Technical Information Service (NTIS), Springfield, Virginia 22161. This document is also available from the Federal Aviation Administration William J. Hughes Technical Center at <a href="http://actlibrary.tc.faa.gov">actlibrary.tc.faa.gov</a> .		
19. Security Classif. (of this report) Unclassified		20. Security Classif. (of this page) Unclassified		21. No. of Pages 33	22. Price

## Contents

<b>1</b>	<b>Introduction.....</b>	<b>1</b>
<b>2</b>	<b>Approach .....</b>	<b>1</b>
2.1	Kinetics.....	3
2.2	Thermodynamics .....	5
<b>3</b>	<b>Experimental .....</b>	<b>7</b>
3.1	Materials.....	7
3.2	Methods .....	8
3.2.1	Fire calorimetry.....	8
3.2.2	Microscale combustion calorimetry.....	8
<b>4</b>	<b>Results and discussion .....</b>	<b>8</b>
<b>5</b>	<b>Conclusions.....</b>	<b>20</b>
<b>6</b>	<b>References.....</b>	<b>20</b>

## Figures

Figure 1. Transient temperature histories for ignition and burning .....	2
Figure 2. Surface temperature and mass flux histories .....	3
Figure 3. Proposed relationship between surface temperature and mass loss rate temperature .....	5
Figure 4. Surface temperature and heat release rate histories for black cast PMMA .....	9
Figure 5. Surface, ignition and burning temperatures of black cast PMMA .....	10
Figure 6. Surface temperature and heat release rate histories for PEEK in cone calorimeter .....	11
Figure 7. Surface, ignition and burning temperatures of PEEK .....	12
Figure 8. Molecular-level ignition and burning resistance .....	13
Figure 9. Integral temperatures T5%, T95% vs. differential temperatures T1, T2.....	15
Figure 10. MCC data for PC/ABS showing temperatures on Q(T) integral.....	16
Figure 11. Fire growth capacities of the polymers in Table 2 .....	18
Figure 12. Expected UL 94V classification vs. <i>FGC</i> of the polymers in Table 2 .....	19
Figure 13. Expected results for 14 CFR 25 heat release rate vs. <i>FGC</i> .....	20

## **Tables**

Table 1. Polymers of this study.....	7
Table 2. Fire Growth Capacities of the polymers in Table 1.....	16

## Acronyms

Acronym	Definition
ABS	Acrylonitrile Butadiene Styrene
ASTM	American Society for Testing and Materials
BPC-CE	Cyanate Ester of Bisphenol-C
BPC-PC	Polycarbonate of Bisphenol-C
CFR	Code of Federal Regulations
FAA	Federal Aviation Administration
FEP	Fluorinated Ethylene Propylene
FGC	Fire Growth Capacity
HDPE	High Density Polyethylene
HIPS	High Impact Polystyrene
MCC	Microscale Combustion Calorimeter
PA66	Polyhexamethylenedipamide
PAI	Polyamideimide
PBI	Polybenzimidazole
PBO	Polybenzobisoxazole
PC	Polycarbonate of Bisphenol-A
PEEK	Polyetheretherketone
PEI	Polyetherimide
PEKK	Polyetherketoneketone
PEN	Polyethylenenaphthalate
PET	Polyethyleneterephthalate
PI	Polyimide
PMMA	Polymethylmethacrylate
POM	Polyoxymethylene
PP	Polypropylene
PPS	Polyphenylene sulfide
PPSU	Polyphenylsulfone
PS	Polystyrene
PSU	Polysulfone
PVC	Polyvinyl Chloride
PVDF	Polyvinylidene Fluoride

<b>Acronym</b>	<b>Definition</b>
TA	Thermal Analysis
UL	Underwriters Laboratories

## **Executive summary**

A model for the fire response of charring and non-charring combustible solids at the continuum (kg) level was used to identify the temperatures at ignition and burning at the molecular level, so that they could be conveniently measured in a micro ( $10^{-6}$  kg) scale combustion calorimeter. The fire response model shows that flame spread is driven by the combustion heat of the fuel gases and follows a path of least thermal resistance (ignition or burning) in the solid. This is the physical basis for an intrinsic, molecular-level, flammability parameter called the Fire Growth Capacity (*FGC*), which can be measured in a microscale combustion calorimeter using milligram samples. The *FGC* spans three orders of magnitude for the combustible solids examined in this study and successfully ranks 30 polymers according to their expected fire performance in bench- and full-scale fire tests.

# 1 Introduction

The heat produced by combustion of fuel gases generated during the burning of polymeric solids in a fire begins with thermally-induced cleavage of primary/covalent chemical bonds between constituent atoms of the molecule, and culminates with the reaction of volatile decomposition products with oxygen in a diffusion flame to produce heat. The arrangement and composition of atoms in the solid (i.e., the molecular architecture) determines whether bond recombination (charring) or bond scission (gas forming) reactions are thermodynamically favored during thermal decomposition, but it is the rate of these chemical reactions coupled with heat and mass transfer at the continuum level that largely determines the fire hazard of a material.

The influence of molecular architecture on the rates of fuel generating reactions can be decoupled from heat/mass transfer using reactive molecular dynamics simulations [1-4], molar group contributions to thermodynamic combustion properties [5-8], and direct correlation with micro ( $10^{-6}$  kg) scale reaction rates and thermodynamic properties measured by thermal analysis (TA) [9-11]. Many of the thermodynamic and kinetic parameters obtained from TA are molecular-level properties that are used in finite element pyrolysis models to simulate burning at bench (kg) scale [11-20] and full ( $10^3$  kg) scale [18].

Another approach has been to parameterize transient fire response at the continuum level, using time-averaged fire behavior in bench-scale fire calorimeters [21-25]. These bench (kg) scale fire response parameters have proven useful for qualitative ranking of material fire performance in flame and fire tests [25-30] and at full-scale [31-32]. Fire response parameters measured at the micro ( $10^{-6}$  kg) scale in TA experiments have also been used to rank the fire performance of materials at the continuum level in flame and fire tests [27-29,33-37]. To date, these micro-scale heat release parameters have been moderately successful at ranking bench-scale burning/heat release rates in forced flaming combustion [36], but they do not include ignitability, or account for the effects of heat and mass transfer in the solid, or reaction kinetics in the flame, which are operative in bench scale flame and fire tests [29,33-35]. This study proposes a micro/molecular scale flammability parameter that includes ignitability, and is therefore expected to be a better predictor of pass/fail tests of flame spread than micro-scale heat release alone.

## 2 Approach

Figure 1 is a schematic diagram of the transient, one-dimensional temperature profiles  $T(x,t)$  for ignition and burning of a non-charring and a charring polymer as they are thought to occur in a fire calorimeter exposed to a constant external heat flux (irradiance) at time  $t = 0$ . The

consecutive processes of ignition and burning lead to the establishment of a surface flame and the development of a pyrolysis zone of thickness  $d$  that moves through the solid at velocity  $v$ , generating fuel gases that mix with oxygen and combust in the surface flame. The pyrolysis zone is bounded by the burning temperature  $T_{burn}$  at the surface  $x = 0$  and by onset pyrolysis/ignition temperature  $T_{ign}$  at depth at  $x = d$ .

Figure 2A and 2B show idealized surface temperature  $T(0,t)$  and mass flux  $\dot{m}''$  histories for the burning model of Figure 1 for a polymer slab subjected to a constant external heat flux,  $\dot{q}''_{ext}$  at time  $t = 0$ , and initial temperature  $T(0,0) = T_0$ . The mass flux approaches the minimum (critical) value for piloted ignition  $\dot{m}''_{ign}$  at surface temperature,  $T_{ign}$ , at which point ( $t_{ign}$ ) a pre-mixed volume of fuel and air ignites. A diffusion flame is established on the surface and the incident heat flux increases to  $\dot{q}''_{ext} + \dot{q}''_{flame}$ . At this point ( $t_{burn}$ ) the mass flux and surface temperature increase to  $\dot{m}''_{burn}$  and  $T_{burn}$ , respectively.

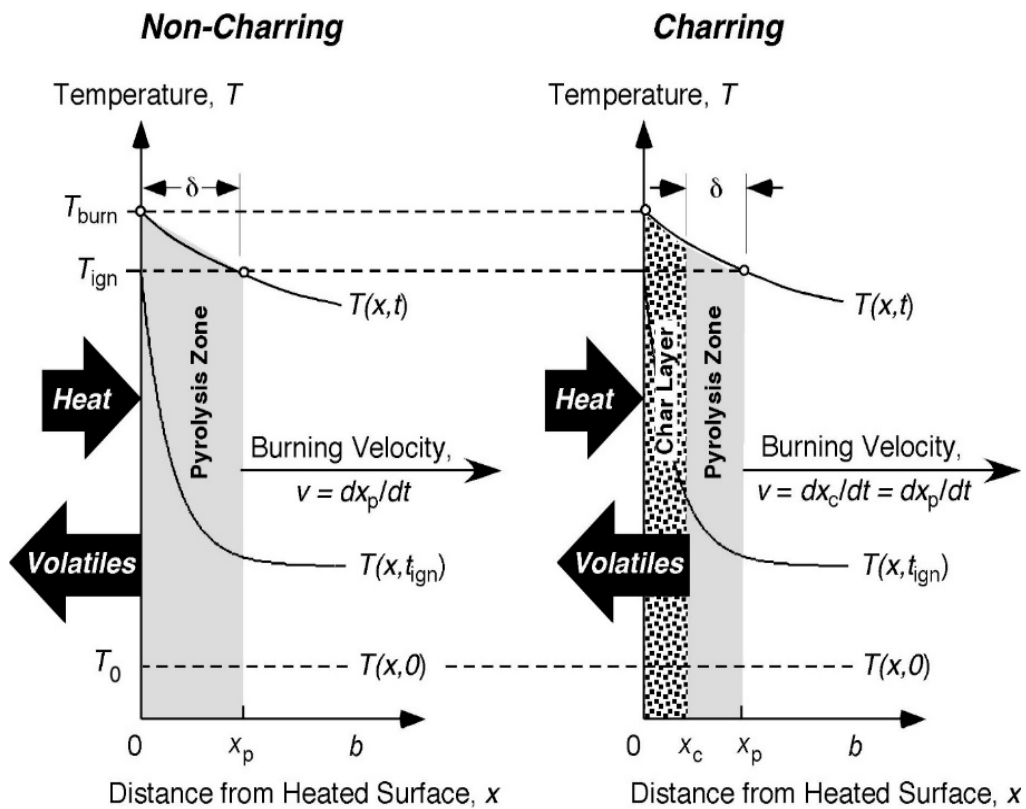


Figure 1. Transient temperature histories for ignition and burning

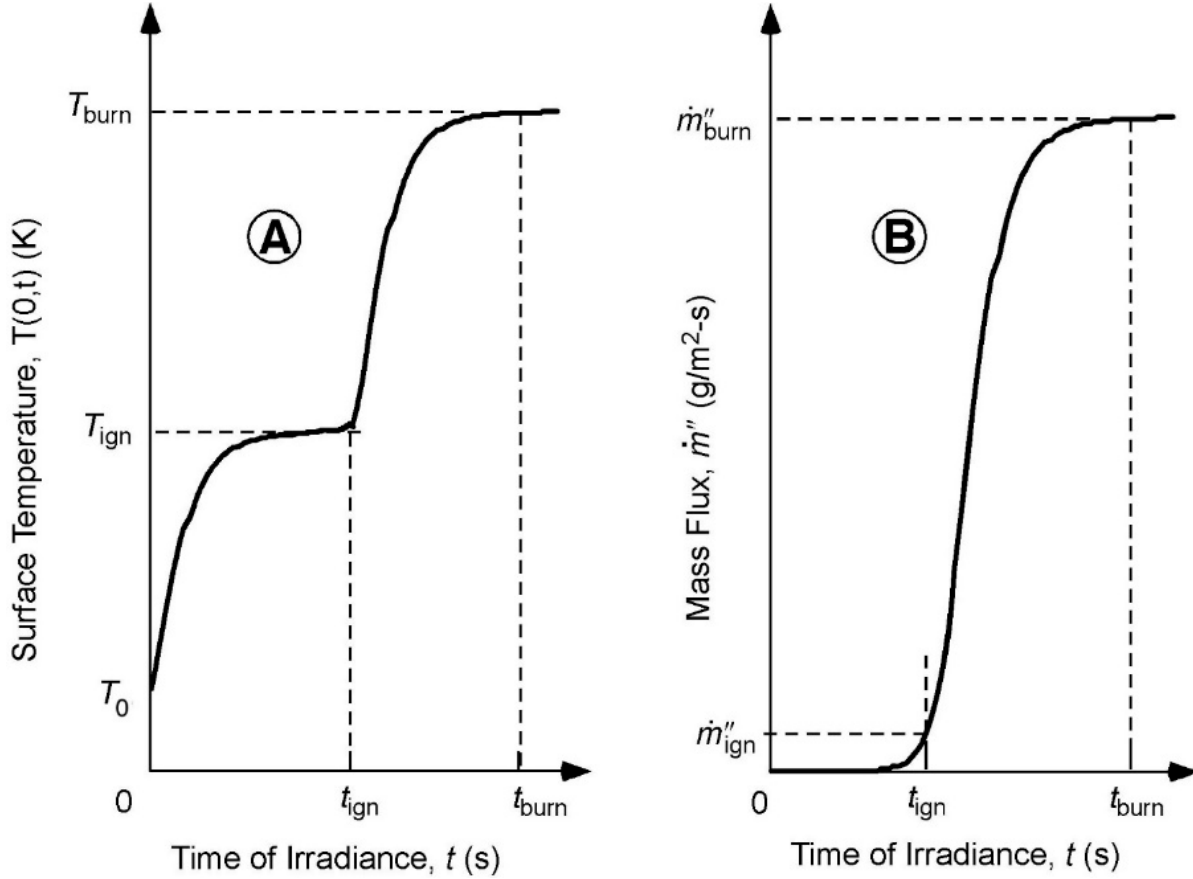


Figure 2. Surface temperature and mass flux histories

## 2.1 Kinetics

The volumetric mass loss rate ( $\text{kg}/\text{m}^3\text{-s}$ ) in the pyrolysis zone at position  $x$ , time  $t$ , is  $\dot{m}_l''' = r(x,t)k(x,t) = r(x,t)A\exp[-E_a/RT(x,t)]$ , with  $A$  and  $E_a$  the frequency factor and activation energy of the thermal decomposition reaction. Conservation of mass for the pyrolysis volume gives the mass/fuel flux ( $\text{kg}/\text{m}^2\text{-s}$ ) exiting the surface  $x = 0$  at temperature  $T_{\text{burn}}$  from a specimen of thickness,  $b$ ,

$$\dot{m}''(t) = (\rho v)_0 - \int_0^b \rho(x,t)A \exp\left[-\frac{E_a}{RT(x,t)}\right] dx \int_\delta^0 \rho(x,t)A \exp\left[-\frac{E_a}{RT(x,t)}\right] dx \quad 1$$

Once a diffusion flame is established, and ignition is sustained, a pyrolysis zone of thickness  $d$  moves through the solid at velocity  $v$  generating gaseous fuel. Each infinitesimal particle of material in the pyrolysis zone will experience a temperature history characterized by an average rate of temperature rise,  $\Delta T/\Delta t \gg v(T_{\text{burn}}-T_{\text{ign}})/d = \dot{m}''(T_{\text{burn}}-T_{\text{ign}})/r d \gg 1\text{K/s}$  for a typical mass flux

( $5 \times 10^{-3} \text{ kg/m}^2\text{-s}$ ), temperature difference ( $T_{\text{burn}} - T_{\text{ign}} = 200\text{K}$ ), density ( $1100 \text{ kg/m}^3$ ), and pyrolysis zone thickness ( $10^{-3} \text{ m}$ ). Assume that a particle in the pyrolysis zone of a burning polymer can be represented by a milligram sample in a nonisothermal analysis experiment at constant heating rate  $\mathbf{b} = \Delta T/\Delta t$ , and that the fraction of solid fuel that has been converted to gaseous products at temperature  $T$  is  $\mathbf{a}$ , a dimensionless variable that ranges from 0 to 1 over the course of the pyrolysis reactions. In this case, the ignition temperature ( $T_{\text{ign}}$ ) and fuel exhaustion temperature ( $T_{\text{burn}}$ ) would correspond to a temperature  $T_1$  at  $\mathbf{a} \gg 0$  and  $T_2$  at  $\mathbf{a} \gg 1$ , respectively. These temperatures are determined by the short-term thermal stability ( $T_1$ ) and thermal decomposition chemistry ( $T_2$ ) of the molecule. In a micro-scale thermal analysis experiment at constant heating rate  $\mathbf{b}$  in which the reaction rate  $d\mathbf{a}/dt$  is measured,  $T_1$  and  $T_2$ , will be solutions to the isokinetic relationship [38],

$$\frac{T}{\beta} \frac{d\mathbf{a}}{dt} = T \frac{d\mathbf{a}}{dT} = \frac{d\mathbf{a}}{d \ln[T]} = 1 \quad 2$$

Figure 3 shows hypothetical surface temperatures at ignition ( $T_{\text{ign}}$ ) and burning ( $T_{\text{burn}}$ ) in a fire calorimeter (3A), as well as the temperatures at incipient pyrolysis ( $T_1$ ) and fuel exhaustion ( $T_2$ ) in a constant heating rate TA experiment (3B). The equivalence of  $T_{\text{burn}}$  and  $T_2$  is based on the assumption that an infinitesimal particle in the pyrolysis zone of a fire calorimeter sample experiences a similar temperature and mass loss history as a milligram sample in a thermal analysis experiment, so the onset and endpoint temperatures of the fuel generating reaction are similar. Note that the open circles in Figure 3B indicate isokinetic temperatures.

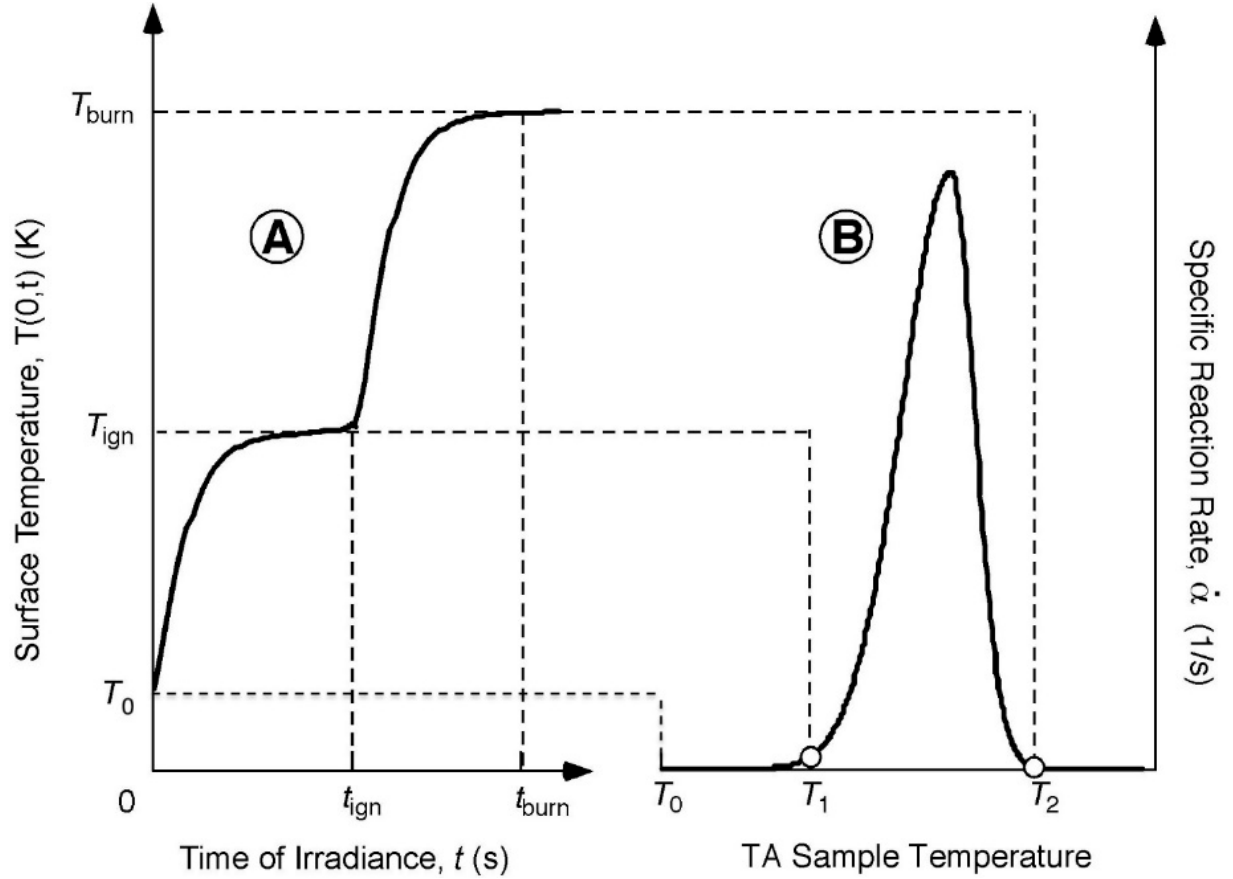


Figure 3. Proposed relationship between surface temperature and mass loss rate temperature

## 2.2 Thermodynamics

The specific energy (J/kg) required to melt and thermally decompose the solid and vaporize the pyrolysis products is [21-24]

$$H_g = c\Delta T_{gas} + L_g \quad 3$$

In Equation 3,  $c$  is the heat capacity of the sample (J/kg-K) and  $\Delta T_{gas} = T_{burn} - T_0$  is the temperature increase above ambient ( $T_0$ ) over which the sample is heated, thermally decomposed, and gasified. If  $f_{ign} = c\Delta T_{gas}/H_g = c\Delta T_{gas}/(L_g + c\Delta T_{gas})$  is the fraction of  $H_g$  stored as sensible heat at burning, and  $f_{burn} = L_g/(L_g + c\Delta T_{gas})$  is the fraction of  $H_g$  that is absorbed by the thermal decomposition process during burning (latent heat), a lower bound estimate of the thermal resistance to gasification in a fire,  $\Delta T_{LB}$  using  $f_{ign}$  and  $f_{burn}$  as weighting factors for ignition and burning, respectively, would be

$$\frac{1}{\Delta T_{LB}} = \frac{\phi_{ign}}{\Delta T_{ign}} + \frac{\phi_{burn}}{\Delta T_{burn}} \quad 4$$

In Equation 4,  $\Delta T_{ign} = T_{ign} - T_0$  is the temperature increase above ambient at ignition, and  $\Delta T_{burn} = T_{burn} - T_{ign}$  is the burning (gasification) temperature interval as per Figure 1. Since,  $f_{ign} + f_{burn} = 1$ , Equation 4 becomes,

$$\frac{1}{\Delta T_{LB}} = \frac{c\Delta T_{gas}/(c\Delta T_{gas} + L_g)}{\Delta T_{ign}} + \frac{L_g/(c\Delta T_{gas} + L_g)}{\Delta T_{burn}} \quad 5$$

It has been shown experimentally that  $c\Delta T_{gas} \gg L_g$  [39], so the fire compliance of a combustible material having fire resistance,  $\Delta T_{fire}$ , can be written,

$$\frac{1}{\Delta T_{fire}} \equiv \frac{1}{\Delta T_{LB}/2} = \frac{1}{\Delta T_{burn}} + \frac{1}{\Delta T_{ign}} \quad 6$$

Multiplying Equation 6 by the effective heat of combustion of the fuel gases,  $H_c$  gives an expression for the amount of heat released by combustion per degree of temperature rise through the processes of ignition and burning in a fire,

$$\frac{H_c}{\Delta T_{fire}} = \frac{H_c}{\Delta T_{ign}} + \frac{H_c}{\Delta T_{burn}} \quad 7$$

The continuum-level fire growth parameter, Equation 7, can be evaluated at micro-scale by recognizing that the specific heat of complete combustion is,  $Q_c \gg (1-m)H_c/c$ , where  $m$  is the mass fraction of char that remains after burning,  $c$  is the combustion efficiency of the fuel gases in a diffusion flame, and  $T_1 = T_{ign}$  and  $T_2 = T_{burn}$  are micro-scale temperatures at the onset and completion of the fuel generation process, respectively, in a nonisothermal experiment at constant heating rate,

$$FGC \equiv \frac{Q_c}{T_1 - T_0} + \frac{Q_c}{T_2 - T_1} \quad 8$$

It has been shown by experiment that  $T_1 \gg T_{ign}$  [42], but it remains to be shown experimentally that  $T_2 \gg T_{burn}$ , so that the intrinsic flammability parameter  $FGC$  can be measured at micro-scale, and that  $FGC$  is a robust predictor of the fire performance of combustible materials at bench- and full-scale.

## 3 Experimental

### 3.1 Materials

The materials tested in this study are listed in Table 1. These are natural, unfilled polymers with minimal processing aids obtained from manufacturers or distributors as extruded profiles, cast sheets, or fibers. Two research polymers [46], the cyanate ester of bisphenol-C (BPC-CE) and the polycarbonate of bisphenol-C (BPC-PC), were also included in the study. The fire and combustion properties of all of the polymers in Table 1 have been reported previously [12-16, 22, 27-30, 37, 42-50]. However, the *FGC* of these polymers is new to this study. Gases used for fire calorimetry and microscale combustion calorimetry were ultra-high purity grades (>99.99%) obtained from local suppliers.

Table 1. Polymers of this study

<b>Polymer</b>	<b>Symbol</b>	<b>Polymer</b>	<b>Symbol</b>
High Density Polyethylene	HDPE	Poly- <i>para</i> -aramid	KEVLAR
Polystyrene (crystal, food grade)	PS	Polyphenylsulfone	PPSU
Polypropylene	PP	Polyvinyl chloride (rigid)	PVC
High Impact Polystyrene	HIPS	Polyetheretherketone	PEEK
Acrylonitrile Butadiene Styrene	ABS	Polyetherimide	PEI
Polyhexamethyleneadipamide	PA66	Polyetherketoneketone	PEKK
Polymethylmethacrylate*	PMMA	Fluorinated ethylene propylene	FEP
Polycarbonate of Bisphenol-A	PC	Phenol formaldehyde thermoset	Phenolic
Blend of PC/ABS (50/50)	PC/ABS	Polybenzobisoxazole	PBO
Polyethyleneterephthalate	PET	Polyamideimide	PAI
Polyethylenenaphthalate	PEN	Polybenzimidazole	PBI
Polyvinylidene fluoride	PVDF	Polyimide	PI
Polyoxymethylene	POM	Cyanate Ester of Bisphenol-C	BPC-CE
Polysulfone	PSU	Polycarbonate of Bisphenol-C	BPC-PC
Polyphenylene sulfide	PPS	Poly- <i>meta</i> -aramid	Nomex

\* PMMA tested from extruded sheet of linear polymer (transparent) and cast sheet (black)

## 3.2 Methods

### 3.2.1 Fire calorimetry

Experiments were conducted in triplicate on a non-charring polymer (black cast PMMA) and a charring polymer (PEEK) in a bench scale fire calorimeter (Cone 1, Fire Testing Technologies). Monolithic solid samples, having dimensions 10cm x 10cm x 0.3cm (PEEK) or 10cm x 10cm x 0.6 cm (black cast PMMA), were subjected to external heat fluxes above the critical values for sustained ignition,  $\dot{q}_{ext}'' = 35 \text{ kW/m}^2$  (PMMA) and  $\dot{q}_{ext}'' = 50 \text{ kW/m}^2$  (PEEK), according to a standard method [51] using an edge frame holder and electrical igniter positioned 25 mm above the sample surface. Surface temperatures at ignition and sustained burning were measured in separate experiments by manually positioning 0.8-mm diameter Type-K thermocouple beads in the pyrolysis layer at the heated surface until a stable diffusion flame appeared and burning had commenced. Duplicate measurements were performed.

### 3.2.2 Microscale combustion calorimetry

Microscale combustion calorimeter (MCC) experiments were conducted in accordance with the standard Method A of ASTM D7309-19[52]. Samples weighing  $\approx 5\text{mg}$  were heated at a constant rate of temperature rise,  $b = 1 \text{ K/s}$  under a  $\text{N}_2$  purge flow of  $80 \text{ cm}^3/\text{min}$ , and the pyrolysis gases combined with oxygen flowing at  $20 \text{ cm}^3/\text{min}$  in a combustor at  $1173\text{K}$  ( $900^\circ\text{C}$ ) to effect complete combustion in excess oxygen. The heat release rate of the polymer at each sample temperature was computed by oxygen consumption flow calorimetry. Samples of each material were tested in triplicate.

## 4 Results and discussion

The phenomena illustrated in Figure 1 and Figure 2 are demonstrated in Figure 4 for a 6-mm thick sample of black cast PMMA tested in a cone calorimeter, according to the standard method [51], at an external heat flux of  $\dot{q}_{ext}'' = 35 \text{ kW/m}^2$ . The surface temperatures (left ordinate) and heat release rate (right ordinate) were measured in separate experiments and are shown as average values of duplicate experiments versus time after exposure to a constant heat flux of  $35 \text{ kW/m}^2$  (abscissa). A surface temperature,  $T_{\text{ign}} = 550 \pm 20\text{K}$ , is recorded at the time of sustained piloted ignition,  $t_{\text{ign}} = 58 \pm 5\text{s}$ . A surface temperature,  $T_{\text{burn}} = 780 \pm 20\text{K}$ , is recorded at the time of sustained burning,  $t_{\text{burn}} = 75 \pm 5\text{s}$ .

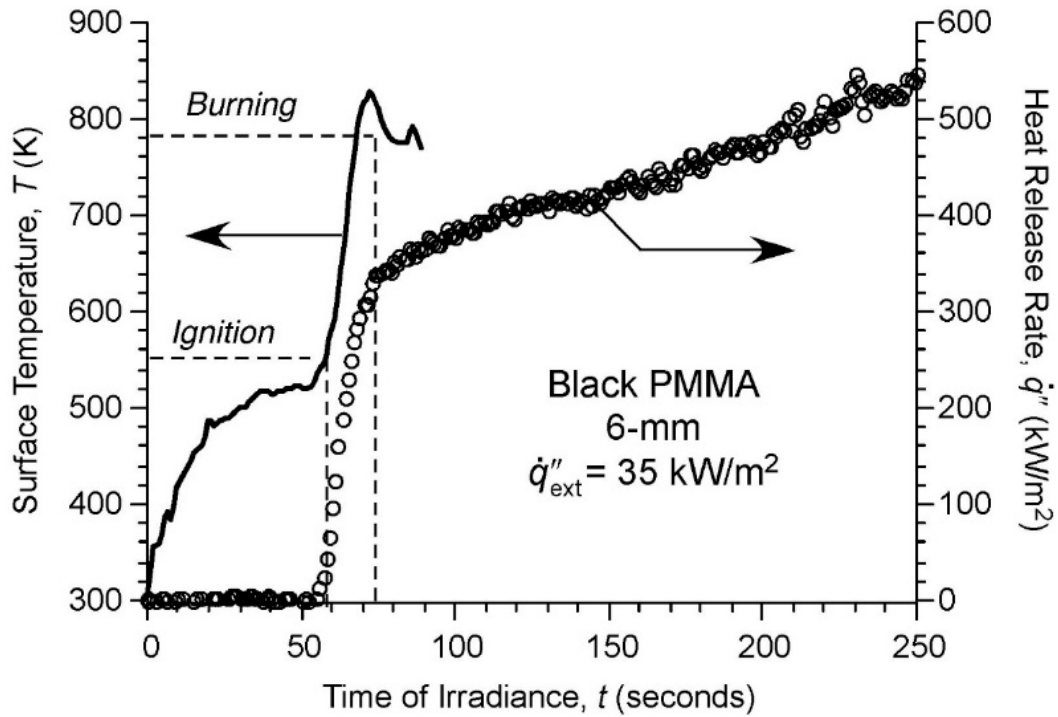


Figure 4. Surface temperature and heat release rate histories for black cast PMMA

Figure 5 shows the ignition and burning temperatures of PMMA in the cone calorimeter from Figure 4 on the left hand side and the specific heat release rate temperatures of PMMA on the right hand side in a MCC experiment at heating rate,  $b = 1\text{K/s}$ . Also shown, as white circles on the specific heat release rate history,  $Q_c(T)$  of PMMA on the right hand side of Figure 5, are the isokinetic temperatures,  $T_1$  and  $T_2$ . These temperatures bracket about 90% of the combustion heat, and about  $2/3$  of the temperature interval between ignition and burning. Open circles on MCC data are isokinetic temperatures.

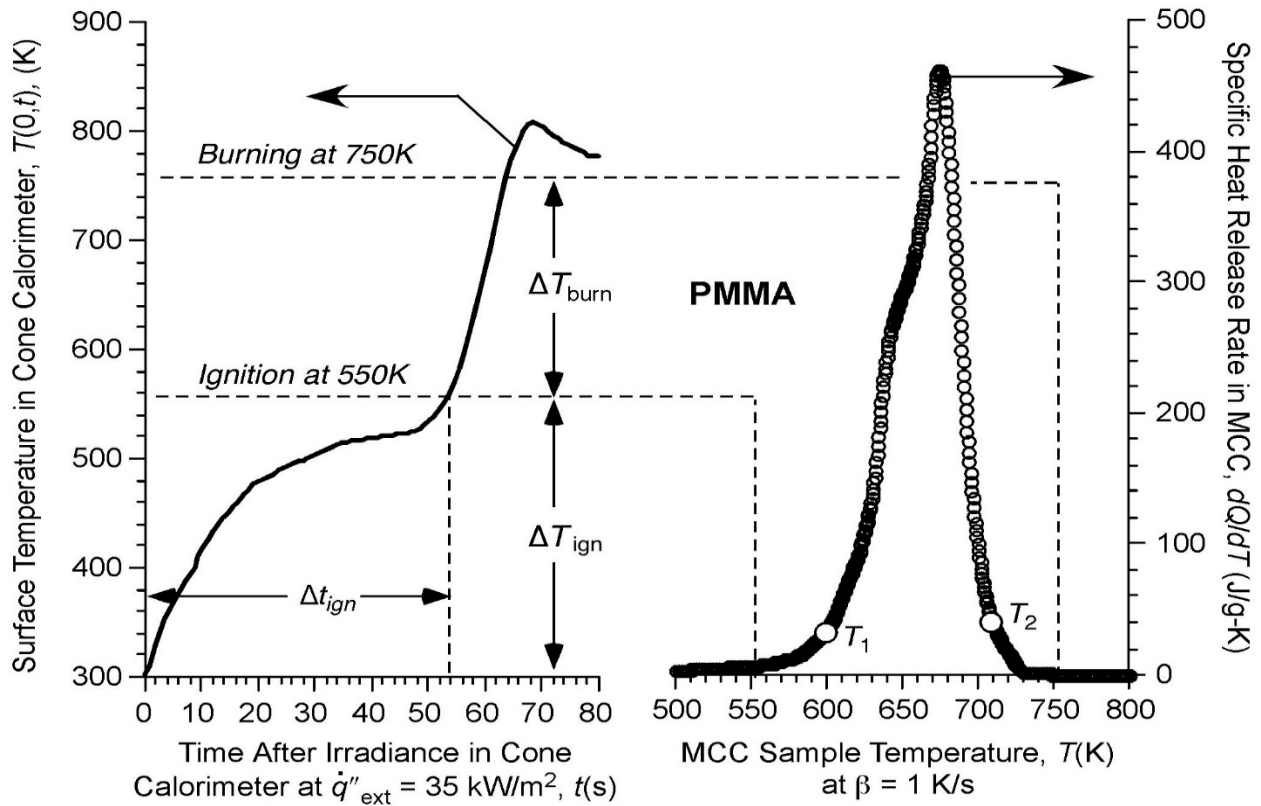


Figure 5. Surface, ignition and burning temperatures of black cast PMMA

Figure 6 shows separate cone calorimeter experiments [49] to measure the surface temperature (left ordinate) and heat release rate (right ordinate) histories of a 10cm x 10cm x 0.3cm sample of the char-forming polymer, polyetheretherketone (PEEK), after exposure to a constant irradiance,  $\dot{q}''_{ext} = 50 \text{ kW/m}^2$  at  $t = 0$  in a cone calorimeter, according to the standard method [51]. The heat release rate of PEEK has a maximum value,  $\dot{q}''_{max} = \Delta H_c \dot{m}''_{burn} \gg 400 \text{ kW/m}^2$  at the measured burning temperature  $T_{burn}$ , after which the surface forms a stable char that is 50% of the original mass and absorbs radiant energy. This causes the heat release rate to decrease significantly due to the temperature gradient through the char,  $T(0)-T(x_c)/x_c$ , which lowers the effective burning temperature from  $T(0) = 1050\text{K}$  to  $T(x_c) = 950\text{K}$ , as shown in the experimental data of Figure 6 and schematically on the right hand side of Figure 1.

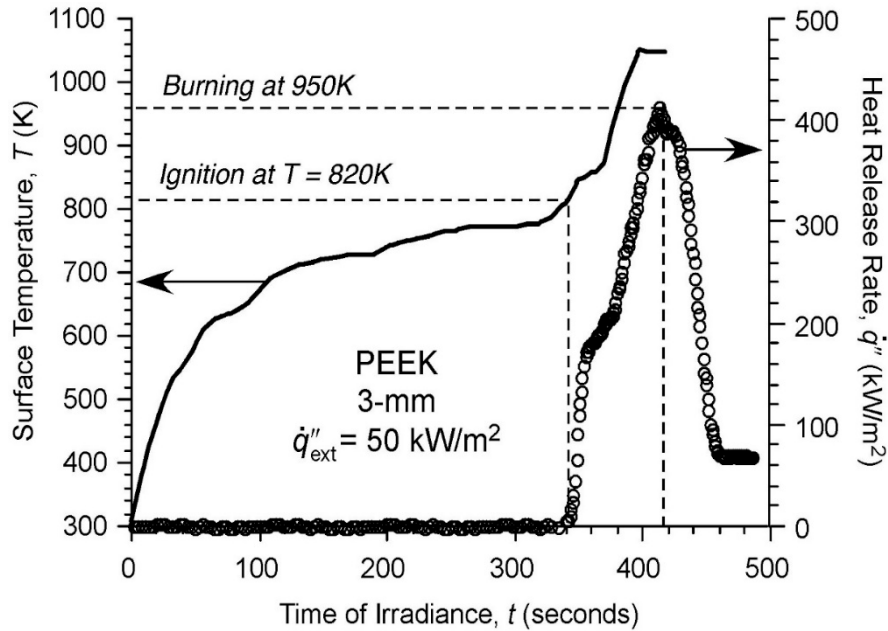


Figure 6. Surface temperature and heat release rate histories for PEEK in cone calorimeter

Figure 7 shows the ignition and burning temperatures of PEEK in the cone calorimeter on the left hand side and the corresponding specific heat release rate temperatures of PEEK on the right hand side for an MCC experiment at a constant heating rate,  $b = 1\text{K/s}$ . Also shown as open circles on the  $Q(T)$  history of PEEK, on the right hand side of Figure 7, are the isokinetic temperatures,  $T_1$  and  $T_2$ . As seen in Figure 5 for PMMA, these temperatures bracket only about 90% of the combustion heat, and about  $2/3$  of the temperature range between ignition and burning. Figure 5 and Figure 7 support the burning model concept of Figure 1 and Figure 2, and the hypothesis that a milligram sample in a micro-scale test experiences a similar temperature and mass loss history as an infinitesimal particle in the pyrolysis zone of a continuum-level cone calorimeter sample.

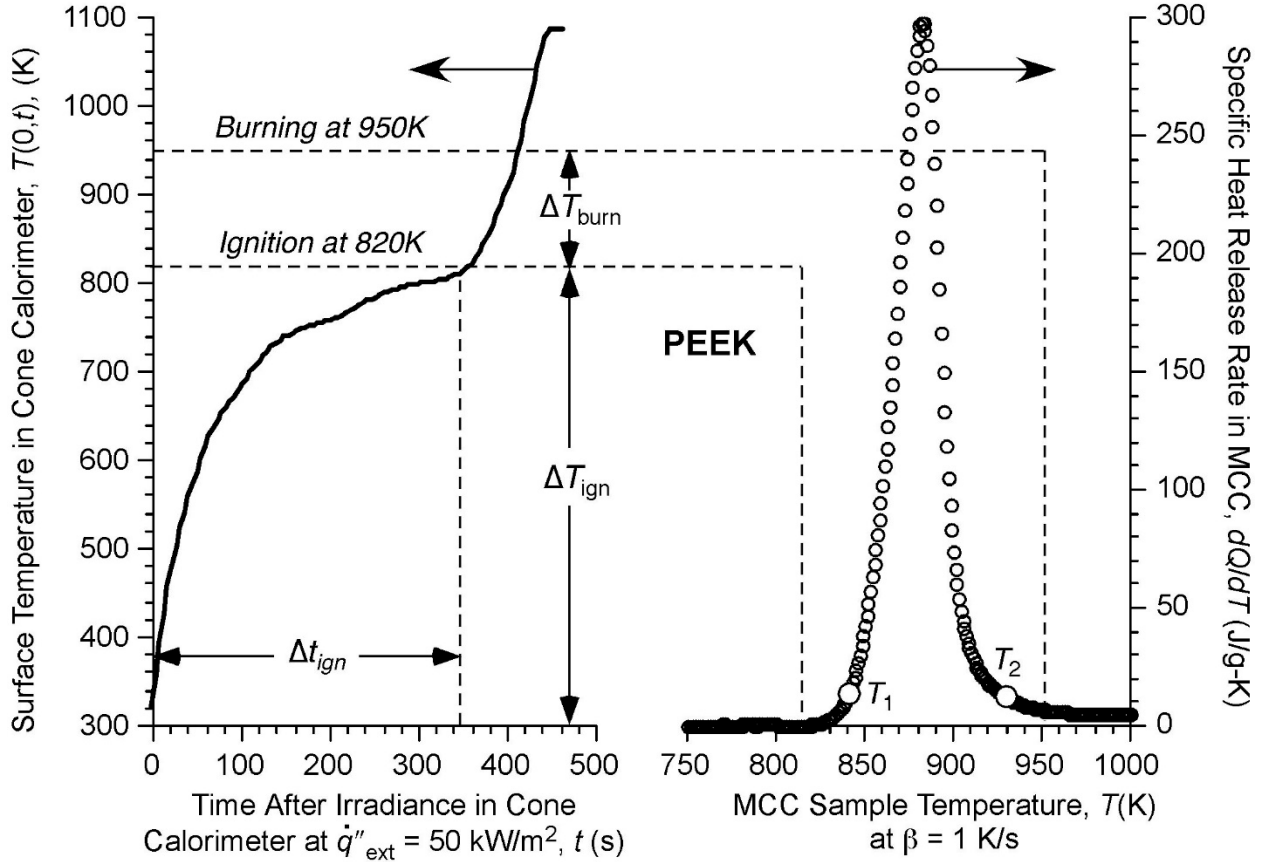


Figure 7. Surface, ignition and burning temperatures of PEEK

Figure 8 is a plot of fire resistance,  $\Delta T_{\text{fire}} = (1/\Delta T_{\text{ign}} + 1/\Delta T_{\text{burn}})^{-1}$  versus thermal decomposition temperature range,  $T_2 - T_0 = (T_2 - T_1) + (T_1 - T_0) = \Delta T_{\text{burn}} + \Delta T_{\text{ign}}$ , of the combustible polymers in Table 1. Figure 8 shows that fire resistance ( $\Delta T_{\text{fire}}$ ) on the ordinate is poorly correlated with thermal decomposition range ( $T_2 - T_0$ ) on the abscissa. This is because fire resistance ( $\Delta T_{\text{fire}}$ ), as defined by Equation 6, is a lower bound of the equally weighted ignition resistance ( $\Delta T_{\text{ign}}$ ) and burning resistance ( $\Delta T_{\text{burn}}$ ), i.e., fire propagation follows the path of least thermal resistance. For this reason, the overall thermal stability of the polymer is less important to fire compliance (propagation) than the relative magnitudes of  $\Delta T_{\text{ign}}$  and  $\Delta T_{\text{burn}}$ , the smaller of which will determine the fire resistance. In particular, the fire resistance  $\Delta T_{\text{fire}}$  is high when both  $\Delta T_{\text{ign}}$  and  $\Delta T_{\text{burn}}$  are large and of similar magnitude, while  $\Delta T_{\text{fire}}$  is low when either of these components of thermal stability is small. This is the physical basis for *FGC* as the propensity for fire growth. In particular, fire propagation of combustible materials is driven by the heat released by combustion of the fuel gases ( $Q_c$ ) and resisted by the thermal barriers to ignition and burning.

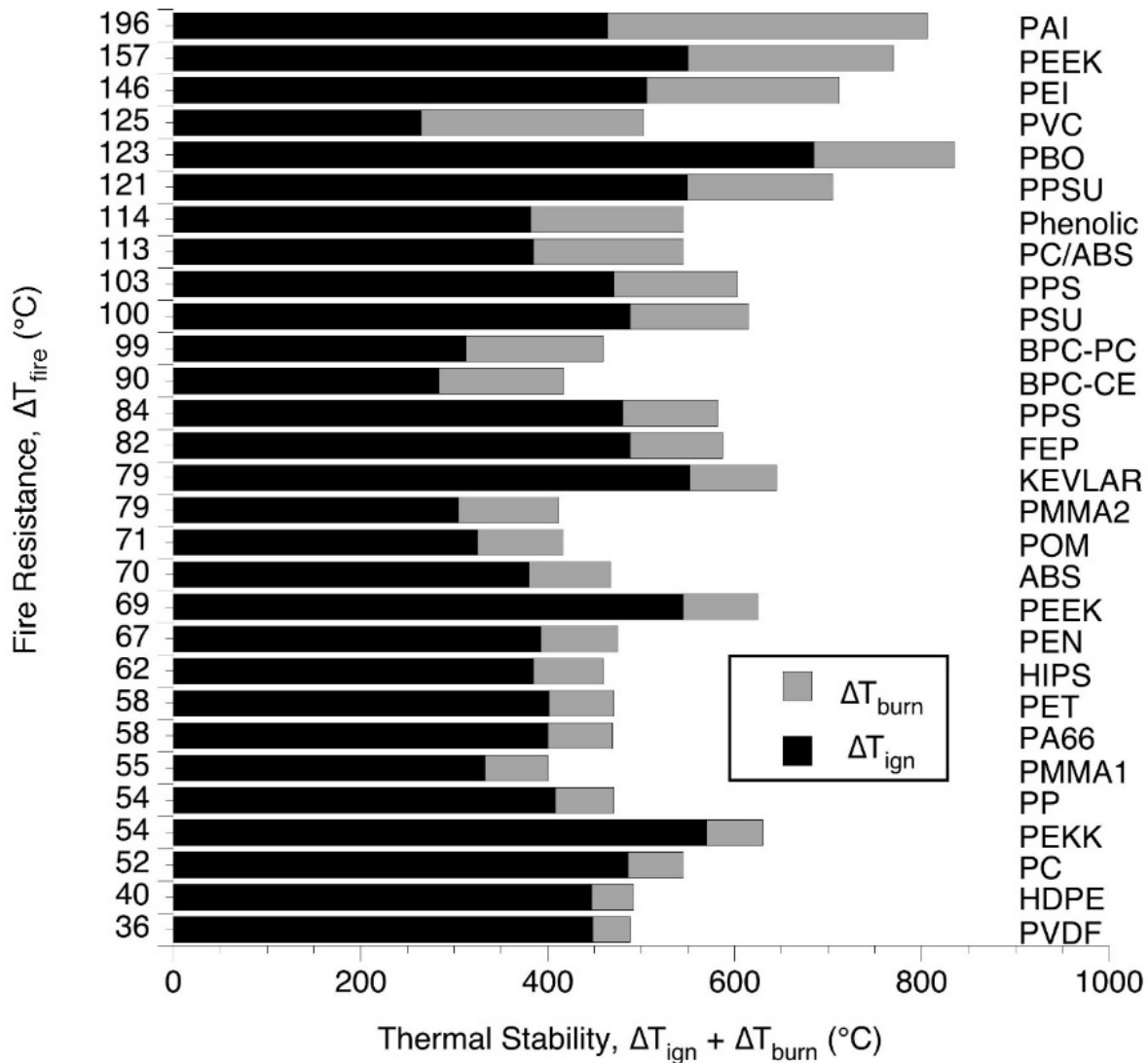


Figure 8. Molecular-level ignition and burning resistance

The qualitative description of the kinetics and energetics of ignition and burning above provides a physical basis and formula for a fire growth parameter measured at milligram scale that captures the processes of fire growth for use in comparing the flammability of materials used in aircraft cabins [53, 54]. Previous studies of MCC parameters and fire performance of materials in standard bench scale flame and fire tests [29] showed that  $Q_c$  and  $h_c = Q_c/(T_2-T_1)$  were the single best predictors of fire performance. Although neither was particularly discriminating in fire tests where ignitability was a contributing factor, or where extrinsic factors associated with thick samples, flame inhibition, or char barrier formation influenced the fire test result, since none of

these are captured by the specific heat release rate measured in the micro ( $10^{-6}$  kg) scale MCC test.

Figure 5 and Figure 7 showed that the kinetic parameters  $T_1$  and  $T_2$  are representative of the temperature range of continuum-level ignition and burning. However, Equation 2 shows that determination of  $T_1$  and  $T_2$  requires an accurate value for the absolute reaction rate measured in the microscale combustion calorimeter,  $d\mathbf{a}/dt = Q\dot{\phi}/Q_c$ , which depends on a good estimate of the zero-point value (baseline),  $Q\dot{\phi} = 0$  from initiation ( $\mathbf{a} = 0$ ) to completion ( $\mathbf{a} = 1$ ) of the fuel generation reaction. Moreover, the isokinetic temperature  $T_2$  is not unique for multi-step reactions with well-resolved maxima and minima in  $Q\dot{\phi}$  an example of which is shown in Figure 10.

To avoid the baseline and uniqueness problems of determining isokinetic  $T_1$  and  $T_2$  directly from the differential curve,  $Q\dot{\phi}$  measured in ASTM D7309-A [52], a standardized integral procedure was adopted in which the onset pyrolysis (ignition) temperature  $T_1$  is taken to be the temperature at  $\mathbf{a} = Q/Q_c = 0.05$ , i.e., the temperature at which 5% of the specific heat of combustion has been released in a constant heating rate microscale combustion calorimeter experiment at  $\mathbf{b} = 1\text{K/s}$ . Likewise, the completion (burning) temperature  $T_2$  is taken to be the temperature at  $\mathbf{a} = Q/Q_c = 0.95$ , i.e., the temperature at which 95% of the specific heat of combustion has been released in the MCC. Figure 9 is a plot of the standard integral temperatures for ignition ( $T_{5\%}$ ) and burning ( $T_{95\%}$ ) versus the corresponding isokinetic differential temperatures,  $T_1$  and  $T_2$ , for the 13 polymers of Table 1 that are shown in the legend. Figure 9 shows that the standard integral burning temperatures,  $T_{95\%}$ , are somewhat higher than the corresponding isokinetic differential temperatures,  $T_2$ , for the thermally-stable, char-forming polymers, PEI, PPSU and PEEK, which undergo a two-step thermal decomposition process, producing about 50% char by weight. This is because combustion of the thermal decomposition products of the char accounts for more than 5% of  $Q_c$ . The standard and isokinetic temperatures of the other 10 polymers in Figure 9 are seen to agree to within the level of approximation,  $T_{\text{ign}} \gg T_1$  and  $T_{\text{burn}} \gg T_2$  in Figure 5, Figure 7 and [42].

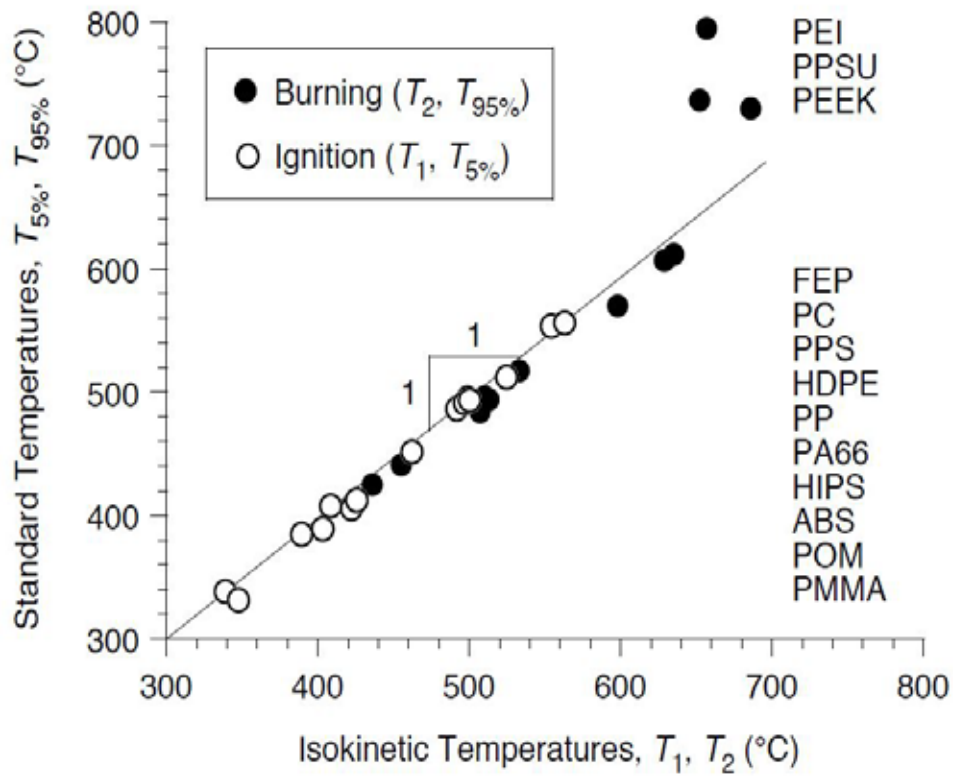


Figure 9. Integral temperatures T5%, T95% vs. differential temperatures T1, T2

Figure 10 shows ASTM D7309-19A data,  $dQ/dT = Q\phi$ , for a 50/50 weight percent blend of polycarbonate/PC and poly(acrylonitrile-butadiene-styrene)/ABS tested in a microscale combustion calorimeter. Solid line in Figure 10 represents the specific heat release rate. Dashed line in Figure 10 represents the fractional heat release.

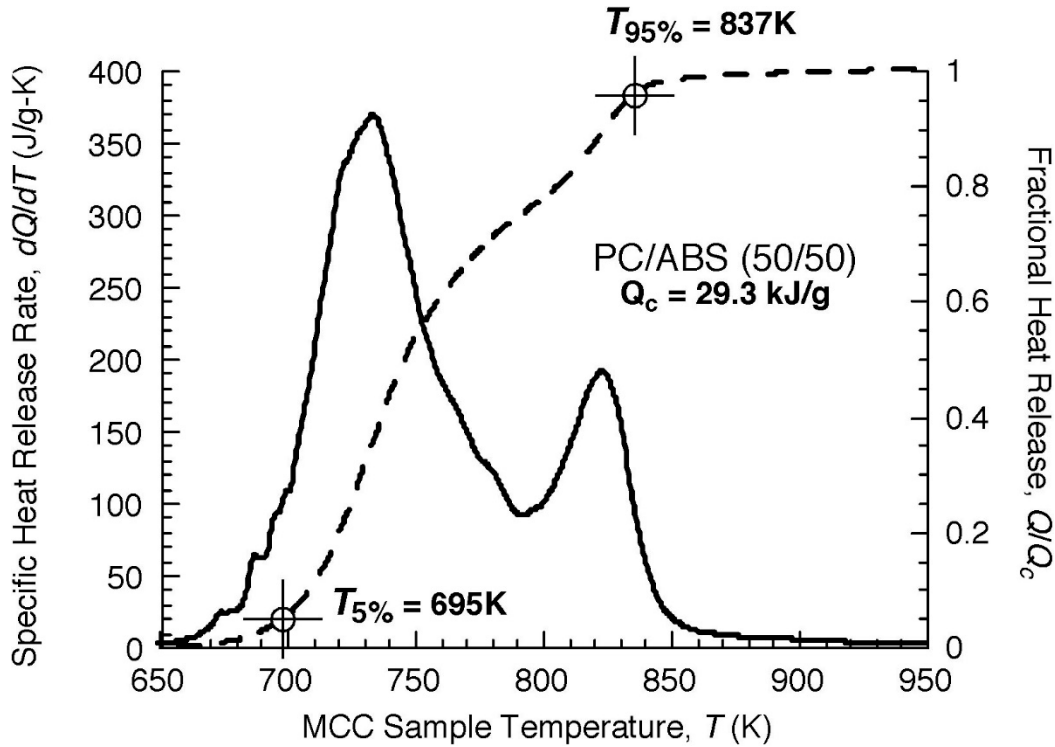


Figure 10. MCC data for PC/ABS showing temperatures on  $Q(T)$  integral

The  $FGC$  is calculated by Equation 8 with temperatures,  $T_{ign} \gg T_1 = T_{5\%}$ , and  $T_{burn} \gg T_2 = T_{95\%}$ ,

$$FGC = \frac{Q_c}{T_{5\%} - T_0} + \frac{Q_c}{T_{95\%} - T_{5\%}} = \frac{Q_c}{(T_{95\%} - T_{5\%})} \frac{(T_{95\%} - T_0)}{(T_{5\%} - T_0)} \quad 9$$

From the data in Figure 10,  $Q_c = 29.3 \text{ kJ/g}$ ,  $T_{ign} \gg T_1 = T_{5\%} = 695\text{K}$ ,  $T_{burn} \gg T_2 = T_{95\%} = 837\text{K}$ , and  $T_0 = 298\text{K}$ , the  $FGC$  for PC/ABS according to Equation 9 is,

$$FGC = \frac{29.3 \text{ kJ/g}}{(837\text{K} - 695\text{K})} \frac{(837\text{K} - 298\text{K})}{(695\text{K} - 298\text{K})} = 280 \text{ kJ/g} - \text{K} = 280 \text{ kJ/g} - ^\circ\text{C}$$

Table 2 is a listing of the Fire Growth Capacities of 30 polymers from  $Q(T)$  measured in accordance with ASTM D7309-19A in the MCC and computed using Equation 9.

Table 2. Fire Growth Capacities of the polymers in Table 1

*PMMA1 = Extruded polymer (clear), PMMA2 = Cast polymer (black)*

<b>Symbol</b>	<b>FGC (J/g-K)</b>	<b>Symbol</b>	<b>FGC (J/g-K)</b>	<b>Symbol</b>	<b>FGC (J/g-K)</b>
HDPE	1031	PET	275	PEI	78
PS	862	PEN	265	PEKK	59
PP	818	PVDF	216	FEP	38
HIPS	607	POM	197	Phenolic	38
ABS	540	PSU	185	PBO	31
PA66	505	PPS	180	PAI	28
PMMA1	437	KEVLAR	130	PBI	22
PC	361	PPSU	100	PI	21
PMMA2	352	PVC	88	BPC-CE	13
PC/ABS	280	PEEK	85	BPC-PC	11

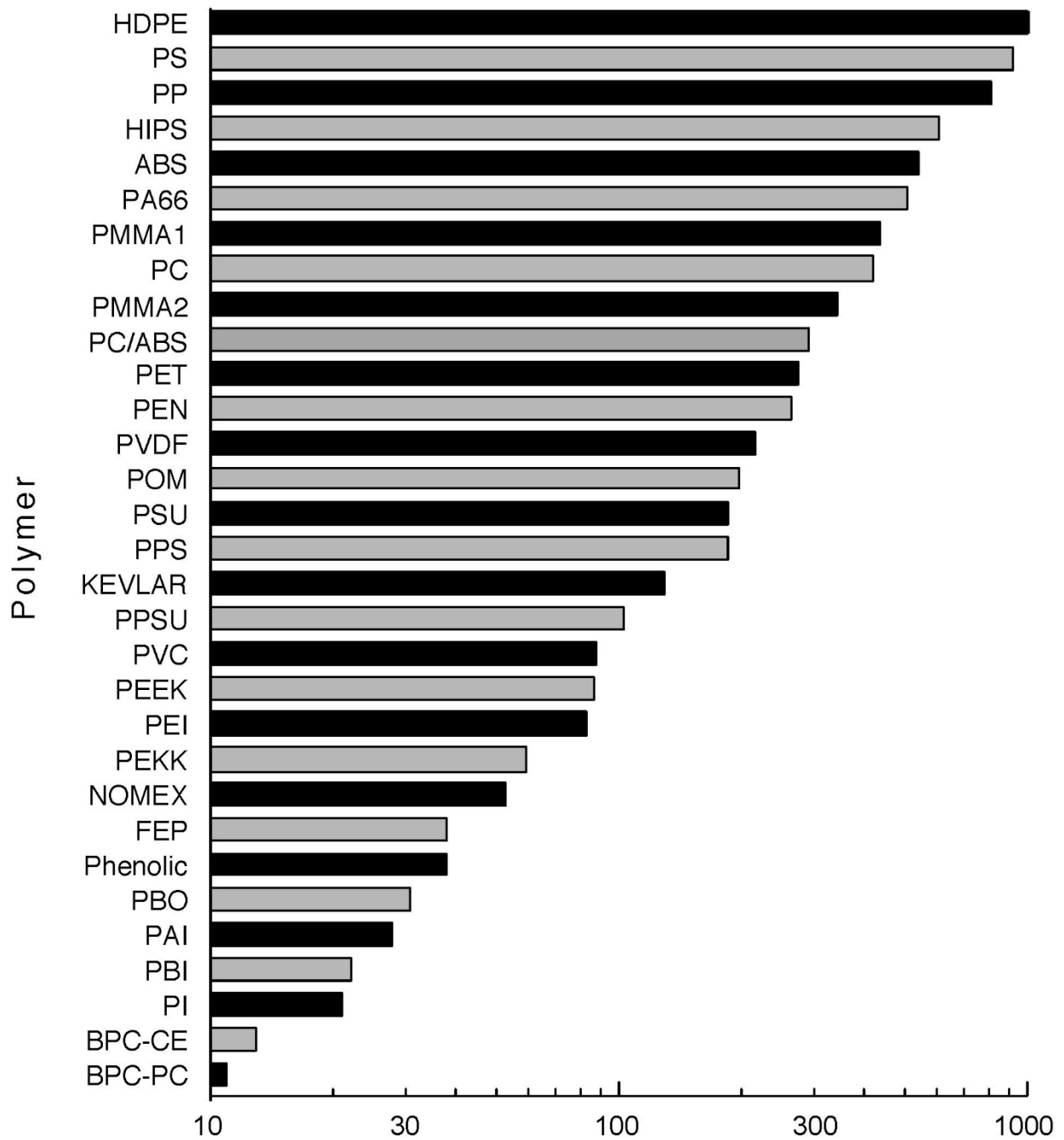


Figure 11. Fire growth capacities of the polymers in Table 2

Figure 11 is a graphical ranking of the *FGC* in Table 2 plotted on a logarithmic scale. Note that the *FGC* of these polymers spans three orders of magnitude, and the *FGC* rank is in general agreement with the observed fire performance of these polymers in bench scale fire and flame tests [27, 28].

Figure 12 is a plot of the expected fire performance and *FGC* of the polymers in upward flame spread, after brief ignition of a vertical, thin prismatic bar (1.6mm x 13mm x 127mm) by a small flame [55,56]. Fire test performance in Figure 12 for the polymers of Table 1 is based on Underwriters Laboratories (UL) classifications in product data sheets, on-line databases, and in the literature for unmodified polymers.

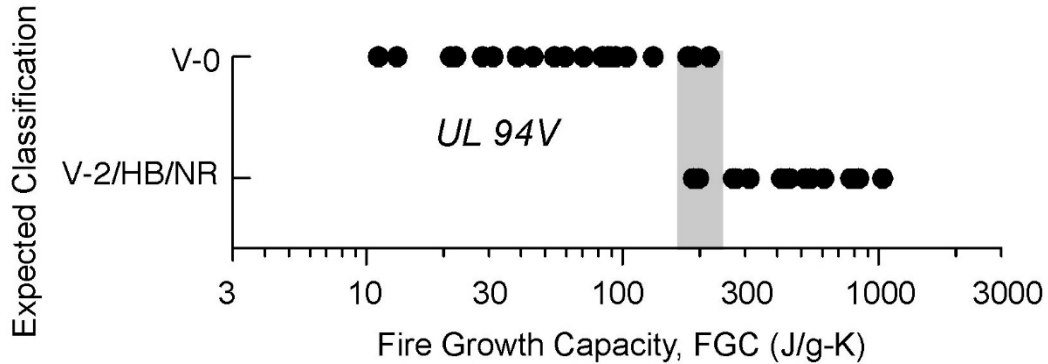


Figure 12. Expected UL 94V classification vs. *FGC* of the polymers in Table 2

Figure 13 is a plot of expected fire performance and *FGC* of the polymers in the Code of Federal Regulations, Part 25 test for peak heat release rate of aircraft materials in a vertical orientation in a fire calorimeter exposed to a pilot flame and radiant heat at  $\dot{q}_{ext}'' = 35 \text{ kW/m}^2$  [57,58]. This test involves simultaneous upward spread and in-depth burning after forced localized ignition by a small premixed flame. A passing result in 14 CFR 25 was assigned to the polymers in Table 2 if they met either of the following conditions:

- The measured peak heat release rate of samples, having dimensions 150mm x 150mm and thickness 1.5mm or 3mm, was less than the FAA limit of  $65 \text{ kW/m}^2$
- The critical heat flux (CHF) for piloted ignition measured in a cone calorimeter in a horizontal orientation in accordance with ASTM E 1354 [51] exceeded the incident heat flux  $\dot{q}_{ext}'' = 35 \text{ kW/m}^2$  in 14 CFR 25 [21-30, 47-49].

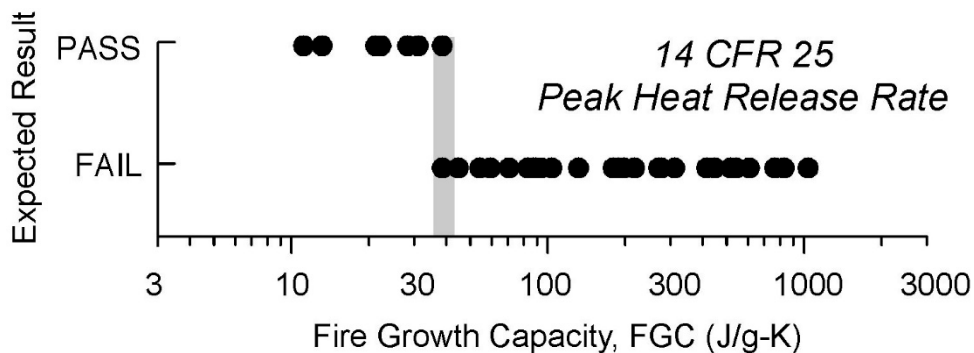


Figure 13. Expected results for 14 CFR 25 heat release rate vs. *FGC*

## 5 Conclusions

A conceptual model supported by experimental data for the fire response of charring and non-charring polymers was used to relate the ignition and burning temperatures at the continuum (kg) level to the temperatures over which fuel is generated at the molecular level in a micro ( $10^{-6}$  kg) scale combustion calorimeter. The assumption that fire propagation is driven by the heat released by the flame ( $Q_c$ ), and follows a path of least thermal resistance ( $\Delta T_{\text{ign}}$  or  $\Delta T_{\text{burn}}$ ), is the physical basis for an intrinsic, molecular-level, flammability parameter called the Fire Growth Capacity (*FGC*), which spans three orders of magnitude and successfully ranks 30 polymers according to their expected fire performance in bench- and full-scale fire tests.

## 6 References

1. Stoliarov, S.I., Westmoreland, P.R., Nyden, M.R., Forney, G.P., A Reactive Molecular Dynamics Model of Thermal Decomposition of Polymers. I. Poly(methylmethacrylate), *Polymer*, 44(3), 883-894 (2003)
2. Stoliarov, S.I., Nyden, M.R., Lyon, R.E., A Reactive Molecular Dynamics Model of Thermal Decomposition of Polymers. II. Poly(isobutylene), *Polymer*, 45(25), 8613-8621 (2004)
3. Smith, K.D., Stoliarov, S.I., Nyden, M.R., Westmoreland, P.R., RMDff: A Smoothly Transitioning Forcefield-Based Representation of Kinetics for Reactive Molecular Dynamics Simulations, *Molecular Simulation*, 33(4-5), 361-368 (2007)
4. Liu, X., Li, X., Liu, J., Wang, Z., Kong, B., Gong, X., Yang, X., Lin, W., Guo, L., Study of High Density Polyethylene (HDPE) Pyrolysis With Reactive Molecular Dynamics, *Polymer Degradation and Stability*, 104, 62-70 (2014).

5. R.E. Lyon, M.T. Takemori, N. Safronava, S.I. Stoliarov and R.N. Walters, A Molecular Basis for Polymer Flammability, *Polymer*, 50(12), 2608-2617 (2009).
6. R.N. Walters and R.E. Lyon, Molar Group Contributions to Polymer Flammability, *Journal of Applied Polymer Science*, 87, 548-563 (2003).
7. Sonnier, R., Otazaghine, B., Iftene, F., Negrell, C., David, G., Howell, B.A., Predicting Flammability of Polymers from Their Chemical Structure: An Improved Model Based on Group Contributions, *Polymer*, 86, 42-55 (2016).
8. Sonnier, R. Negrell-Guirao, C., Vahabi, H., Otazaghine, B., David, G., Lopez-Cuesta, J.M., Relationships Between the Molecular Structure and Flammability of Polymers: Study of Phosphonate Functions Using Microscale Combustion Calorimetry, *Polymer*, 53(6), 1258-1266 (2012).
9. Mensah, R.A., Jiang, L., Asante-Okyere, S. *et al.* Comparative evaluation of the predictability of neural network methods on the flammability characteristics of extruded polystyrene from microscale combustion calorimetry. *J Therm Anal Calorim* **138**, 3055-3064 (2019).  
<https://doi.org/10.1007/s10973-019-08335-0>
10. Mensah, R.A., Xu, Q., Asante-Okyere, S. *et al.* Correlation analysis of cone calorimetry and microscale combustion calorimetry experiments. *J Therm Anal calorim* 136, 589-599 (2019).  
<https://doi.org/10.1007/s10973-018-7661-5>
11. Agarwal. G., Lattimer, B., Method for Measuring the Standard Heat of Decomposition of Materials, *Thermochemical Acta*, 545, 34-47 (2012).
12. Li J., Stoliarov S. I., Measurement of Kinetics and Thermodynamics of the Thermal Degradation for Non-charring Polymers," *Combustion and Flame*, vol. 160, pp. 1287-1297 (2013).
13. Li J., Stoliarov S. I., Measurement of Kinetics and Thermodynamics of the Thermal Degradation for Charring Polymers, *Polymer Degradation and Stability*, vol. 106, pp. 2-15 (2014).
14. Stoliarov, S.I., Li, J., Parameterization of Pyrolysis Models for Polymeric Materials, *Fire Technology*, 52, 79-91 (2016).
15. Stoliarov S. I., Lyon R. E., Thermo-Kinetic Model of Burning, Federal Aviation Administration Technical Note, DOT/FAA/AR-TN08/17 (2008).
16. Stoliarov S. I., Leventon I. T., Lyon R. E., Two-dimensional Model of Burning for Pyrolyzable Solids, *Fire and Materials*, vol. 38, pp. 391-408 (2014).
17. Lautenberger C., Fernandez-Pello C., Generalized Pyrolysis Model for Combustible Solids," *Fire Safety Journal*, vol. 44, pp. 819-839 (2009).
18. McGrattan K., Hostikka S., McDermott R., Floyd J., Weinschenk C., Overholt K., Fire Dynamics Simulator (Version 6) Technical Reference Guide, National Institute of Standards and Technology Special Publication 1018-6 (2014).
19. Henderson J. B., Wiebelt J. A., Tant M. R., A Model for the Thermal Response of Polymer

- Composite Materials with Experimental Verification, *Journal of Composite Materials*, vol. 19, pp. 579–595 (1985).
20. Vovelle C., Delfau J. L., Reuillon M., Bransier J., Laraqui N., Experimental and Numerical Study of the Thermal Degradation of PMMA, *Combustion Science and Technology*, vol. 53, pp. 187-201 (1987).
  21. Tewarson, A., Pion R.F., Flammability of Plastics-I. Burning Intensity, *Combustion and Flame* 26, 85-103 (1976).
  22. A. Tewarson, Generation of Heat and Chemical Compounds in Fires, in SFPE Handbook of Fire Protection Engineering, 3<sup>rd</sup> Edition; Society of Fire Protection Engineers, Boston, MA, Section 3, 2002, pp 82-161.
  23. A. Tewarson, Flammability Parameters of Materials: Ignition, Combustion and Fire Propagation, *Journal of Fire Sciences*, 12(4), 327-408 (1994).
  24. A. Tewarson, Flammability, Physical Properties of Polymers Handbook, J.E. Mark, Ed., AIP Press, NY, 1996, pp. 577-604.
  25. R.E. Lyon, S. Crowley and R.N. Walters, Steady Heat Release Rate by the Moment Area Method, *Fire and Materials*, 32, 199-212 (2008)
  26. J.G. Quintiere, A Theoretical Basis for Flammability Properties, *Fire and Materials*, 30(3), 175-214 (2006).
  27. R.E. Lyon and M.L. Janssens, *Polymer Flammability*, Encyclopedia of Polymer Science & Engineering (on-line edition), John Wiley & Sons, New York, NY, October 2015.
  28. R.E. Lyon, *Plastics and Rubber*, in Handbook of Building Materials for Fire Protection, C. A. Harper, Ed., McGraw-Hill, New York, Chapter 3, pp. 3.1-3.51, 2004.
  29. R.E. Lyon, N. Safronava, J.G. Quintiere, S.I. Stoliarov, R.N. Walters and S. Crowley, Material Properties and Fire Test Results, *Fire and Materials*, 38, 264-278 (2014).
  30. A. Tewarson, M. Kahn, P.K. Wu, and R.G. Bill, Flammability Evaluation of Clean Room Polymeric Materials for the Semiconductor Industry, *Fire and Materials*, 25, 31-42 (2001).
  31. R.V. Petrella, The Assessment of Full-Scale Fire Hazards from Cone Calorimeter Data, *Journal of Fire Sciences*, 12, 14-43 (1994).
  32. Ostman, B.A.L. and Nussbaum, R.M., 1989. Correlation Between Small-scale Rate Of Heat Release And Full-scale Room Flashover For Surface Linings. *Fire Safety Science* 2: 823-832
  33. R.E. Lyon and N. Safronava, A Probabilistic Analysis of Pass/Fail Fire Tests, Federal Aviation Administration Final Report DOT/FAA/TC-12/13, October 2013.
  34. N. Safronava and R.E. Lyon, Combustion Characteristics of Adhesive Compounds Used in the Construction of Aircraft Cabin Materials, Federal Aviation Administration Final Report, DOT/FAA/TC-TN12/12, July 2012.

35. J.G. Qunitiere, B.P. Downey and R.E. Lyon, An Investigation of the Vertical Bunsen Burner Test for Flammability of Plastics, Federal Aviation Administration Report DOT/FAA/AR-TN11/19, February 2012.
36. R.E. Lyon, R.N. Walters and S.I. Stoliarov, A Thermal Analysis Method for Measuring Polymer Flammability, *Journal of ASTM International*, 3(4), 1-18 (2006).
37. R.E. Lyon, R.N. Walters, S.I. Stoliarov, and N. Safronava, Principles and Practice of Microscale Combustion Calorimetry, Federal Aviation Administration Technical Report, DOT/FAA/TC-12/53, Revision 1, 2014.
38. R.E. Lyon, Isokinetics, *Journal of Physical Chemistry, Part A*, 123, 2462-2469 (2019).
39. S.I. Stoliarov and R.N. Walters, Determination of the Heats of Gasification of Polymers Using Differential Scanning Calorimetry, *Polymer Degradation and Stability*, 93(2) (2008).
40. D. Drysdale, An Introduction to Fire Dynamics (3<sup>rd</sup> Edition), John Wiley & Sons, Chichester, UK, 2011.
41. J.G. Quintiere, *Fundamentals of Fire Phenomenon*, John Wiley & Sons, Chichester, UK, 2006.
42. R.E. Lyon, N. Safronava and S. Crowley, Thermal Analysis of Polymer Ignition, *Fire and Materials*, 42, 668-679 (2018).
43. R.E. Lyon and J.G. Quintiere, Piloted Ignition of Combustible Solids, *Combustion & Flame*, 151, 551-559 (2007).
44. S.I. Stoliarov, N. Safronava N, R.E. Lyon, The Effect of Variation in Polymer Properties on the Rate of Burning, *Fire and Materials*, 33, 257-271 (2009).
45. R.E. Lyon and T. Emrick, Non-halogen Fire Resistant Plastics for Aircraft Interiors, *Polymers for Advanced Technologies*, 19, 609-619 (2008).
46. R.E. Lyon, L. Speitel, R. Filipczak, R. Walters, S. Crowley, S.I. Stoliarov, L. Castelli and M. Ramirez, Fire Smart DDE Polymers, *High Performance Polymers*, 19 (3), 323-355 (2007).
47. R.E. Lyon, S. Gandhi, and S. Crowley, Fire Properties of Heat-Resistant Polymers, Technical Note DOT/FAA/TC-TN18/32, Federal Aviation Administration, June 2019.
48. Safronava N, Stoliarov SI, Lyon RE. Effect of Moisture on Ignition of Polymers, *Fire Technology* 2015; 51(5): 1093-1112.
49. E.S. Oztekin, S.B. Crowley, R.E. Lyon, S.I. Stoliarov, P. Patel, and T.R. Hull, Sources of Variability in Fire Test Data: A Case Study on Poly(aryletheretherketone)(PEEK), *Combustion and Flame* 2012; 159: 1720-1731.
50. R.E. Lyon and S.A. Crowley, Fire Properties from Unsteady Burning, 13<sup>th</sup> International Symposium on Fire Safety Science, Waterloo, Canada, April 27-May 1, 2020.
51. ASTM Standard E1354-13. Test Method for Heat and Visible Smoke Release Rates for Materials and Products Using and Oxygen Consumption Calorimeter, American Society for Testing and Materials, West Conshohocken, PA. 2013.

52. ASTM Standard D7309-19, Standard Test Method for Determining Flammability Characteristics of Plastics and Other Solid Materials Using Microscale Combustion Calorimetry, ASTM International, West Conshohocken, PA, 2019.
53. R.E. Lyon, Materials With Reduced Flammability in Aerospace and Aviation, Advances in Fire Retardant Materials, A.R. Horrocks and D. Price, Eds., Chapter 20, CRC Press, Boca Raton, FL, 2008.
54. R.E. Lyon, R.N. Walters, N. Safronava, Small Scale Fire Test for Component Substitutions in Aircraft Cabin Materials, Interflam19, Sussex, UK, July 1-3, 2019.
55. Flammability of Plastic Materials, Northbrook, IL: Underwriters Laboratories Inc., 1991, UL 94 Section 2 (Horizontal: HB), and Section 3 (Vertical: V-0/1/2).
56. Standard Test Method for Measuring Comparative Burning Characteristics of Solid Plastics in a Vertical Position, ASTM D3801-06, American Society for Testing and Materials (International), West Conshohocken, PA, 2006.
57. Code of Federal Regulations, Title 14 Aeronautics and Space, Chapter 1 Federal Aviation Administration, Department of Transportation, Part 25 Airworthiness Standards: Transport Category Airplanes, Section 853 Compartment Interiors, U.S. Government Printing Office, Washington, D.C.,
58. Aircraft Materials Fire Test Handbook, April Horner, Ed., Federal Aviation Administration Final Report, DOT/FAA/AR-00/12, 2000.